

On the robustness of emptying filling boxes to sudden changes in the wind

John Craske^{1†} and Graham O. Hughes¹

¹Department of Civil and Environmental Engineering, Imperial College London,
London SW7 2AZ, UK

(Received ?; revised ?; accepted ?. - To be entered by editorial office)

We determine the smallest instantaneous increase in the strength of an opposing wind that is necessary to permanently reverse the forward displacement flow that is driven by a two-layer thermal stratification. With an interpretation in terms of the flow's energetics, the results clarify why the ventilation of a confined space with a stably-stratified buoyancy field is less susceptible to being permanently reversed by the wind than the ventilation of a space with a uniform buoyancy field. For large opposing wind strengths we derive analytical upper and lower bounds for the system's marginal stability, which exhibit a good agreement with the exact solution, even for modest opposing wind strengths. The work extends a previous formulation of the problem (Lishman & Woods 2009, *Building and Env.* **44**, pp. 666-673) by accounting for the transient dynamics and energetics associated with the homogenisation of the interior, which prove to play a significant role in buffering temporal variations in the wind.

1. Introduction

1.1. Background

In contrast to indoor conditions that are controlled mechanically, naturally ventilated spaces surrender themselves to the forces and fluctuations of their surrounding environments (see e.g. Linden 1999). In addition to the prediction of the steady state of a system, one should therefore be concerned with its robustness or its propensity to switch abruptly to an alternative steady state.

In the specific case of an indoor space subjected to a source of heating and an external wind load, the governing equations admit multiple steady state solutions (Hunt & Linden 2005). The solutions correspond to either *forward flow* or *reverse flow*, for which unidirectional discharge occurs through the opening at the top or bottom of the space, respectively. From an operational point of view it is necessary to consider the transient route towards these steady states from time-dependent governing equations (Kaye & Hunt 2004; Coomaraswamy & Caulfield 2011). The analysis of the system's transient behaviour leads naturally to questions relating to the sensitivity and robustness of steady states to random or controlled variations in design or environmental conditions.

There exist reverse flows that are unstable, in the sense that infinitesimal changes in the wind load will cause a dramatic change in the system's state. In contrast, there exist locally stable reverse and forward flows that are insensitive to infinitesimal changes in the wind. Finite changes in the wind, however, can result in a transition between stable forward flow and stable reverse flow, and provide the motivation for the present study.

Previous work (Yuan & Glicksman 2008; Lishman & Woods 2009) has determined the

† Email address for correspondence: john.craske07@imperial.ac.uk

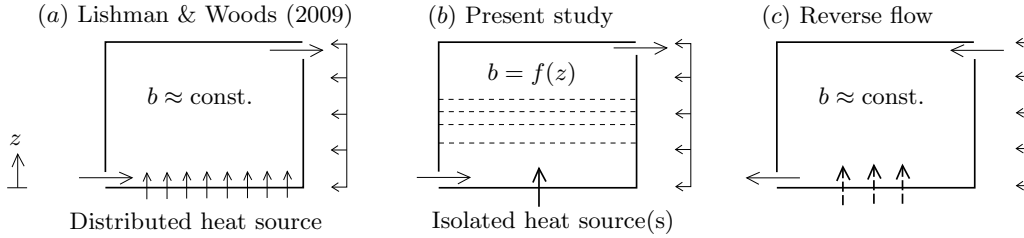


FIGURE 1. The ventilation driven by (a) a well-mixed interior of uniform buoyancy and (b) a stably-stratified interior. Schematic (c) illustrates reverse flow, for which the interior is well mixed and assumed to be of uniform buoyancy.

minimum instantaneous amount by which the strength of an opposing wind must increase to force a transition from forward flow to reverse flow, under the assumption of a base state consisting of uniform buoyancy. Given that isolated sources of buoyancy and heterogeneous boundary conditions result in spatially non-uniform distributions of buoyancy (see e.g. Linden *et al.* 1990), we relax the assumption of uniform buoyancy and quantify the extent to which the destruction of a stratified interior modifies the system's robustness to fluctuations in the wind.

1.2. An illustration of the general problem

Consider a volume with low- and high-level openings, as depicted in figure 1. In (a), following Lishman & Woods (2009), the heating of the space is distributed evenly over the floor and the resulting buoyancy field is assumed to be uniform. In (b), which is the starting point for the present work, the heating occurs unevenly over localised sources to produce a buoyancy field that is non-uniform (i.e. stratified). Ventilation of the space is driven by pressure differences resulting from the average internal buoyancy and external forces arising from the wind. In a steady state, the rate at which buoyancy drains from the top of the space is equal to the rate at which it is supplied to the space in the form of heat, which we assume to be the same in figures 1(a)-(c).

The average buoyancy and ventilation rate is greater in (a) than in (b) (see e.g. Gladstone & Woods 2001, p. 307). To understand why, note that the ventilation rate increases with pressure difference across the upper opening, which in turn increases with average buoyancy in the volume. For a given average buoyancy, the buoyancy at the top of the volume in (a) is less than it is for any stable stratification (b); hence the buoyancy flux through the upper opening will only be the same in both cases if the ventilation rate – and therefore the average buoyancy – is maximised in (a).

Figure 1(c) illustrates a situation in which the pressure difference across the space due to wind exceeds the pressure difference created by internal buoyancy. The resulting flow is in the reverse direction and is accompanied by an approximately well-mixed interior of uniform buoyancy, regardless of the way in which the space is heated (Hunt & Linden 2005). In a steady-state, the average buoyancy in (c) is necessarily less than the average buoyancy in (b) and, therefore, less than the average buoyancy in (a).

A transient increase in the opposing wind strength can cause a transition from forward flow to reverse flow. The question that our work addresses is whether the minimum increase in the wind strength that is required for the transition is greater for system (a) than it is for system (b). Whilst the required reduction in average buoyancy is greater for system (a), we show that the wind must perform additional work over a finite time to destroy the stratification in system (b), making it more robust to fluctuations in the wind than one might otherwise expect.

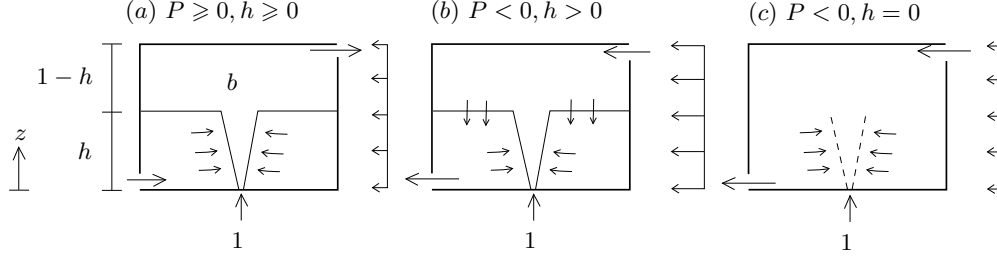


FIGURE 2. Wind-opposed buoyancy driven ventilation resulting in (a): steady forward flow; (b): transient reverse flow with a stratification and (c): steady reverse flow. A sufficiently large increase in the opposing wind results in a transition from (a) to (c).

1.3. Theoretical model

We will assume that buoyancy is introduced from a point source located at the bottom of a domain, whose ventilation is facilitated by low- and high-level openings. For forward flow, the resulting two-layer stratification, illustrated in figure 2(a), is a special example of the stratified environments that were considered in figure 1(b). The state of the system can be described by the dimensionless height of the resulting interface h and the dimensionless uniform buoyancy b of a well-mixed upper layer, which, following Coomaraswamy & Caulfield (2011), are non-dimensionalised using the total domain height and plume buoyancy flux. Following Hunt & Linden (2005), the volume flow rate through the space is determined by the dimensionless pressure difference

$$P = \underbrace{b(1-h)}_{\text{buoyancy}} - \underbrace{W}_{\text{wind}}, \quad (1.1)$$

between the dimensionless stack-driven pressure $b(1-h)$ and the dimensionless wind-induced pressure difference W between the windward and leeward openings, which corresponds to the square of a Froude number based on the wind speed. In adopting this notation, which differs slightly from the explicit use of the Froude number $Fr = \sqrt{W}$ by Hunt & Linden (2005) to express the same physical concepts, we follow Coomaraswamy & Caulfield (2011), in which further details pertaining to the non-dimensionalisation can be found.

In an unsteady state the governing equations comprise statements of volume conservation and buoyancy conservation in the upper layer:

$$\frac{dh}{dt} = \begin{cases} -h^{5/3} + |VP|^{1/2}, & P \geq 0, h \geq 0 \\ -h^{5/3} - |VP|^{1/2}, & P < 0, h > 0 \\ 0, & P < 0, h = 0 \end{cases}, \quad \frac{d}{dt}b(1-h) = \begin{cases} 1 - |VP|^{1/2}b, & P \geq 0, h \geq 0 \\ 1, & P < 0, h > 0 \\ 1 - |VP|^{1/2}b, & P < 0, h = 0 \end{cases} \quad (1.2a,b)$$

respectively, where V is a dimensionless opening area that accounts for discharge coefficients. The $h^{5/3}$ in (1.2a) corresponds to the volume flux in an axisymmetric plume at $z = h$, which would cause the height of the interface to reduce in the absence of the stack-driven discharge $|VP|^{1/2}$. The sub-equations in (1.2) refer to forward displacement ventilation ($P \geq 0, h \geq 0$), reverse displacement ventilation ($P < 0, h > 0$) and reverse mixing ventilation ($P < 0, h = 0$), as depicted in figure 2. If a well-mixed interior of uniform buoyancy is assumed from the outset (as it is in Lishman & Woods 2009), the system's state can be uniquely described by the buoyancy b alone, which evolves according to (1.2b) with $h = 0$.

When W exceeds a critical value $W_c = \sqrt[3]{27/4V}$, the system has three fixed points, at which $d(b, h)/dt = 0$, each corresponding to a different steady-state solution (Hunt & Linden 2005). For $W > W_c$ there are two stable solutions and an unstable steady-state solution

describing reverse flow. Reverse flow is not possible when $W < W_c$ and, as pointed out by Lishman & Woods (2009), stable reverse flow subjected to decreasing wind will jump to displacement ventilation when $W < W_c$.

The fixed point for forward flow (b_0, h_0) through a stratified environment satisfies (1.2) for $P \geq 0$:

$$b_0 = h_0^{-5/3}, \quad V h_0^{-5/3} (1 - h_0) - h_0^{10/3} - VW = 0. \quad (1.3)$$

A fixed point for reverse flow when $W > W_c$ satisfies (1.2b) for $h = 0$ and is therefore a stable or unstable state corresponding to one of two positive real roots of the cubic

$$b^3 - Wb^2 \pm V^{-1} = 0. \quad (1.4)$$

It is useful to regard the two-dimensional phase space for the system, shown in figure 3, as a projection of the space to which states (b, h, W, V) belong. Constant values of V and W correspond to a particular plane or slice through the entire space. The features of phase space that are shown in the projection in figure 3 therefore depend on particular values of V and W , whose axes are hidden from view. Whilst the grey arrows in figure 3(a) correspond to the system's time derivatives when $V = 1$ and $W = 2 > W_c$, we have also included the system's trajectory for other values of W to indicate how the system would evolve if the wind strength were to change.

As discussed in Coomaraswamy & Caulfield (2011), states for which $h > b^{-3/5}$, representing an upper layer whose buoyancy exceeds the buoyancy in the plume at the interface, are beyond the scope of the model equations and therefore not included in figure 3. The phase space is partitioned by a separatrix curve $B_0\text{-}\alpha_0$, which emanates from the unstable fixed point B_0 , into basins of attraction corresponding to the stable fixed points A_0 and C_0 . The fixed point to which a system's state eventually evolves is determined by whether its state lies to the left or to the right of the separatrix curve. The separatrix curve can be obtained by adding a small positive perturbation to $h = 0$ at the unstable fixed point B_0 , to provide initial conditions for the integration of the governing equations *backwards* in time until $h = b^{-3/5}$ at α_0 .

2. Flow reversal

The direction of the flow through the system can be permanently reversed by a sustained increase ΔW in the wind strength. The resulting pressure difference must be larger than the favourable pressure difference created by the upper layer of warm fluid during the transition.

2.1. The critical change in wind speed ΔW_*

If the system's state starts at the fixed point A_0 corresponding to forward flow, a step increase ΔW will cause its state to change. Hereafter we refer to ΔW_* as the minimum increase required to permanently reverse the flow. Thus, for $\Delta W < \Delta W_*$, the system will return to a state corresponding to forward flow (see, for example, the line $A_0\text{-}A_-$ in figure 3(a), projected from the plane $W + \Delta W$). For $\Delta W > \Delta W_*$ the system will transition to a state corresponding to stable reverse flow (see, for example, the line $A_0\text{-}C_+$ in figure 3(a), projected from the plane $W + \Delta W$). Whether a transition to stable reverse flow occurs depends on whether the step increase ΔW moves the separatrix curve at α_0 to the left or to the right of the system's base state A_0 .

The strength of the optimal (minimum) wind increase $\Delta W_* : \alpha_0 \mapsto \alpha_*$ projects the point α_* of the separatrix curve in the $W + \Delta W_*$ plane exactly onto the fixed point A_0 for forward flow corresponding to W , as shown in figure 3(b). The increase would

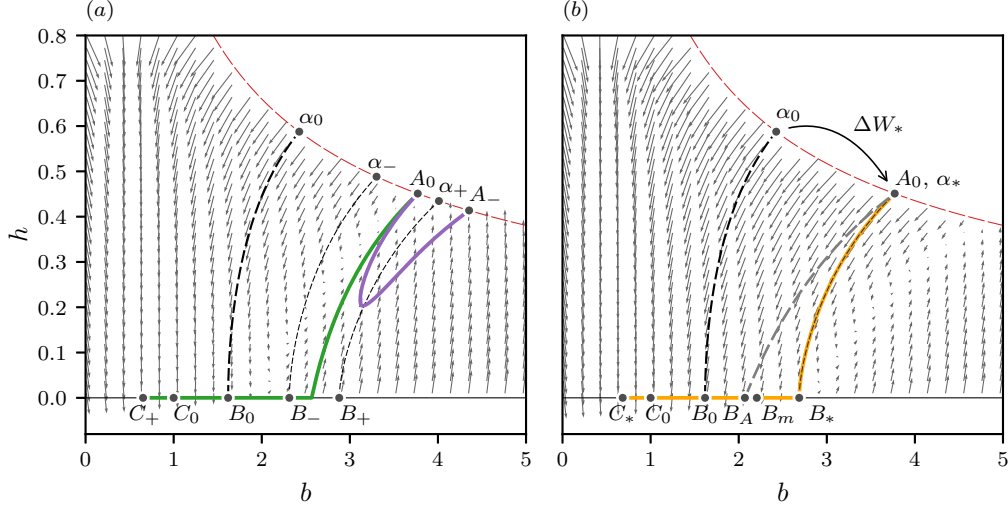


FIGURE 3. The projected phase space for a two-layer stratification with base wind strength $W = 2$ and $V = 1$. The points A_0 , B_0 and C_0 denote the stable (forward flow), unstable and stable (reverse flow) fixed points of the system, respectively. The line $\alpha_0 - B_0$ denotes the separatrix curve for $W = 2$ and $V = 1$. The lines $A_0 - A_-$ and $A_0 - C_+$ in (a) denote the trajectories taken by the system following sub-optimal $\Delta W = 0.5 < \Delta W_*$ and super-optimal $\Delta W = 1.0 > \Delta W_*$ step changes in the wind strength, respectively. The thin dashed lines $\alpha_- - B_-$ and $\alpha_+ - B_+$ denote the position of the separatrix curves for sub- and super-optimal changes in the wind, respectively. The line $A_0 - C_*$ in (b) denotes the trajectory taken by the system following an optimal $\Delta W_* \approx 0.825$ step change in the wind strength, which, for $h > 0$ coincides with the system's separatrix curve $\alpha_- - B_-$ for the wind strength $W + \Delta W_*$. Along $A_0 - B_A$ the average buoyancy $b_0(1 - h_0)$ is constant and B_A corresponds to the location of the unstable fixed point for a sub-optimal step change $\Delta W < \Delta W_*$ in wind strength. The point B_m is the location of the fixed point for forward flow, under the assumption of a well-mixed interior (Lishman & Woods 2009). The grey arrows denote the time derivatives of a given state (b, h) for an opposing wind of strength W in (a) and $W + \Delta W_*$ in (b).

need to be sustained for at least as long as it would take for the system's trajectory to cross the separatrix curve at the unstable fixed point B_0 associated with the base wind strength. No instantaneous increase for which $\Delta W < \Delta W_*$ can reverse the flow because ΔW_* is the smallest step change that places the system's state in the basin of attraction for stable reverse flow in the W plane.

The base wind strength that corresponds to $W + \Delta W_*$ can be found by integrating the governing equations backwards in time along the separatrix curve $B_* - \alpha_*$ from $(b, h) = (b_*, 0)$ for $W + \Delta W_*$, where b_* satisfies a modified version of (1.4):

$$b_*^3 - (W + \Delta W_*)b_*^2 + V^{-1} = 0. \quad (2.1)$$

The point α_* , at which the resulting trajectory intersects the line $h = b^{-3/5}$, corresponds to the steady-state solution A_0 for forward flow for a base wind strength W . Performing the calculation for different values of $W + \Delta W_*$ provides the relationship between W and ΔW_* for marginal stability that is displayed in figure 4.

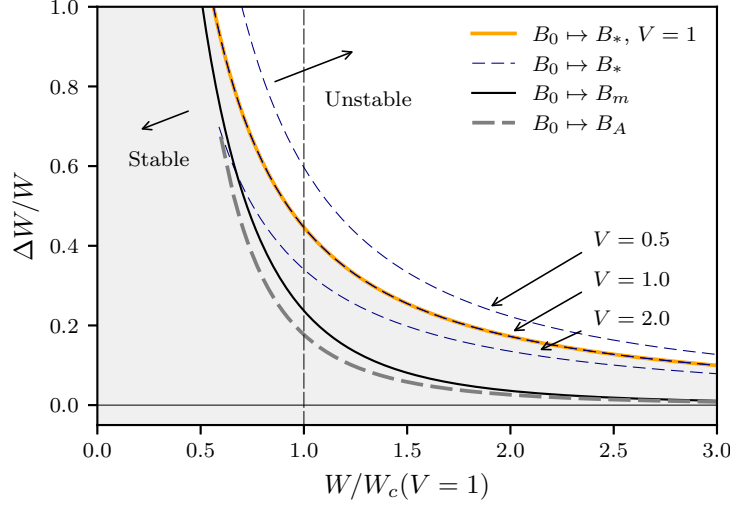


FIGURE 4. Stability diagram indicating instantaneous increases in the wind strength ΔW that cause a reversal of forward ventilation flow. The stable and unstable regions are separated by the minimal instantaneous increase in wind strength ΔW_* : $B_0 \mapsto B_*$ that is necessary to permanently reverse the ventilation of a two-layer stratified interior for an opening parameter $V = 1$ (the dashed lines corresponding to $V = 0.5$ and $V = 2.0$ are included for comparison). The lines in the stable region correspond to the unstratified interior of uniform buoyancy considered by Lishman & Woods (2009), corresponding to B_m in figure 3(b) and the wind increase estimated from the average buoyancy $b_0(1 - h_0)$ of a two-layer stratification, corresponding to B_A in figure 3(b).

2.2. Comparison with Lishman & Woods (2009)

A steady-state forward flow in the environment of uniform buoyancy considered by Lishman & Woods (2009) satisfies (1.2b) with $P \geq 0$ and $h = 0$:

$$b_m^3 - Wb_m^2 - V^{-1} = 0. \quad (2.2)$$

whose real solution corresponds to B_m in figure 3(b). It is evident from figure 3(b) that $b_m < b_*$, where b_* is the buoyancy of the stratified interior's ‘upper’ layer when, during application of the step increase in the wind strength, the interface reaches floor level and the upper layer engulfs the entire space. The minimum increase in the wind necessary to reverse the flow through an initially stratified environment is therefore greater than it is for an environment whose buoyancy is initially uniform. As can be seen in figure 4, for base wind strengths close to $W_c = \sqrt[3]{27/4V}$, the critical increase ΔW_* for a two-layer stratification is approximately twice as large as it is for an interior of uniform buoyancy, for which $\Delta W_* = 2(b_m - W)$ (Lishman & Woods 2009). At larger base wind strengths $W \gg W_c$ a stratified interior can withstand changes in the wind that are an order of magnitude larger than those that can be withstood by an interior of uniform buoyancy.

We have demonstrated that states of uniform buoyancy satisfying (2.2) are less robust to changes in the wind than states consisting of a two-layer stratification satisfying (1.3). As explained in §1.2, given that the average buoyancy of the two-layer stratification is less than the uniform buoyancy satisfying (2.2), we expect estimations of the system’s robustness based on its average buoyancy $b_0(1 - h_0)$ to be misleading and conservative. Indeed, as deduced in §1.2, the line A_0 - B_A on which $b(1 - h) = b_0(1 - h_0)$ is constant in figure 3(b), intersects the horizontal axis $h = 0$ at B_A , where $b = b_0(1 - h_0) <$

b_m . Conclusions about the robustness of stratified environments based on their average buoyancy therefore provide a lower bound on the strength of the minimum destabilising increase in the wind, which suggests that the work required to homogenise a stratified interior plays a crucial role in determining its stability.

Changing the opening parameter V affects neither the qualitative aspects of our results concerning the system's robustness nor our comparisons with interiors of uniform buoyancy. As shown in figure 4, and consistent with intuition, large values of the opening parameter, corresponding to openings with relatively large area, make the stratified interior more susceptible to flow reversal, whilst small values make it more robust. It is interesting that the enhanced robustness afforded by a reduction in V also entails a reduction in the height of the interface of a two-layer stratification.

2.3. Time scale

The transient route that forward displacement flow takes before being permanently reversed by a sufficiently large increase in the wind strength ΔW_* comprises two distinct processes. The first involves lowering the interface of the stratification until the warm upper layer engulfs the entire space (A_0 - B_* in figure 3). The second involves purging warm air from the space via the lower opening, until the system reaches stable equilibrium (B_* - C_* in figure 3). The subject of this section are the time scales on which these processes occur.

The time Δt_* that it takes for the interface to be lowered to floor level can be obtained by numerical integration, backwards in time, along B_* - A_0 , and is displayed in figure 5. A consequence of the discontinuity at $h = 0$ in the governing equations (1.2) is that the time derivatives of b and h are non-zero arbitrarily close to the unstable fixed point B_* . Physically, this corresponds to the fact that the interface descends with a finite speed just before it reaches floor level.

In contrast to the trajectory A_0 - B_* , temporal derivatives tend to zero at both ends of the trajectory B_* - C_* , which makes the time scale associated with the purging of warm air from the space infinite without a perturbation at B_* . Using (1.2) when $P < 0$, $h = 0$, for the modified wind strength $W + \Delta W$, we define a characteristic timescale by noting that $-db/dt$ is maximised when $b = 2(W + \Delta W)/3$; hence

$$\frac{db}{dt} \leq 1 - \left(\frac{W + \Delta W}{W_c} \right)^{3/2}, \quad (2.3)$$

along B_* - C_* . A useful lower bound on the time Δt_0 that it takes for the system to travel along B_* - C_* is therefore

$$\frac{\Delta b}{\left(\frac{W + \Delta W}{W_c} \right)^{3/2} - 1} \leq \Delta t_0. \quad (2.4)$$

where Δb is the difference in buoyancy between the two fixed points for reverse flow from (1.4). The time scale Δt_0 is displayed in figure 5, along with the total time $\Delta t_* + \Delta t_0$. Note that the estimation (2.4) relates to the time taken for the system to reach C_* , and does not, therefore, necessarily provide an indication of the minimum duration for which the increase in wind strength ΔW would be need to be sustained. The latter would involve estimating the time it would take for the system to travel along B_* - B_0 .

The lower bound (2.4) indicates that the time Δt_0 that it takes for the system to travel along B_* - C_* is substantially larger than the time Δt_* that it takes for the system to travel along A_0 - B_* , for the base wind speeds shown in figure 5. Both Δt_* and Δt_0 decrease

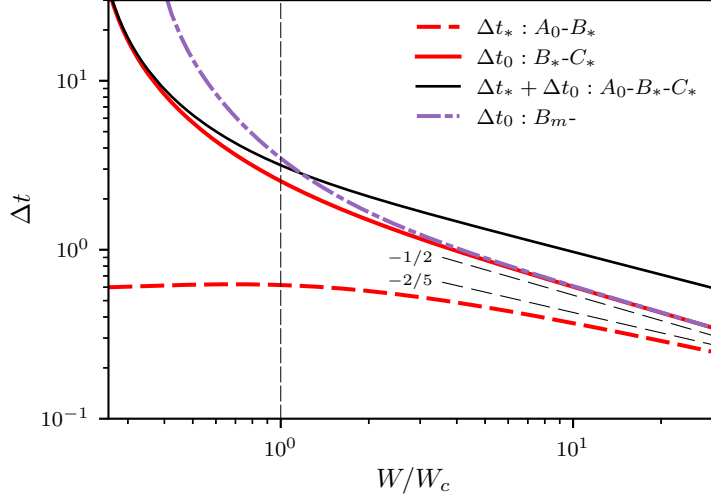


FIGURE 5. Transient time scale associated with lowering the interface of a stratified interior along A_0-B_* in figure 3 (solved numerically) and purging relatively warm well-mixed air from the space along B_*-C_* (estimated using (2.4)). The curve labelled ‘ B_m- ’ corresponds to the timescale estimated from (2.4) for a well-mixed state to move from B_m to stable reverse flow. The thin dashed lines, whose gradients are $-1/2$ and $-2/5$ correspond to the asymptotic scaling of Δt_* and Δt_0 when $W \rightarrow \infty$, as discussed in §3.

with increasing base wind strength W . Consequently, the estimation (2.4) for a well-mixed interior, for which ΔW_* is less than it is for a stratified interior, is always greater than Δt_0 for a stratified interior, although the difference is insignificant for $W/W_c \gtrsim 2$.

To interpret figure 5 from a practical perspective it is useful to note that time in (1.2) is non-dimensionalised using the ‘filling-box’ time scale (Coomaraswamy & Caulfield 2011) $S/(cF^{1/3}H^{2/3})$, where S is the horizontal area of the space, $c = 6\varepsilon/5(9\varepsilon\pi^2/10)^{1/3}$ for an entrainment coefficient ε , F is the buoyancy flux and H is the height of the space. For reference, if $S = 100 \text{ m}^2$, $F = 100 \text{ m}^4\text{s}^{-1}$ (corresponding to a heat load of approximately 3.5 kW), $H = 5 \text{ m}$ and $\varepsilon = 0.1$, the filling box time is approximately one minute, but for a large lecture theatre it could be close to one hour (Linden 1999). With this information in mind, ΔW_* could only be regarded as a ‘gust’ in the wind, for sufficiently small filling box time scales or sufficiently large base wind speeds. It is otherwise more appropriate to regard ΔW_* as arising from a more persistent change in prevailing wind conditions.

3. Bounds on the stability of forward flow

3.1. Exact bounds

To understand the physics and scaling laws behind the stability of forward flow, we consider the trajectory that the system takes through phase space when it is subjected to an optimal increase in wind strength ΔW_* . Rather than retaining the volume flux $h^{5/3}$ in (1.2a), which depends on the unknown and variable interface height h , we assume the volume flux to be equal to the constant $\lambda h_0^{5/3}$, where h_0 is the initial interface height. Incorporation of the volume flux in this way results in a tractable differential equation and facilitates the over and under estimation of the effect that the plume’s volume flux has on the system’s stability. By substituting the solution $b(1-h) = b_* + t$ of (1.2b) into the modified (1.2a) using the buoyancy b_* at the unstable fixed point, one obtains

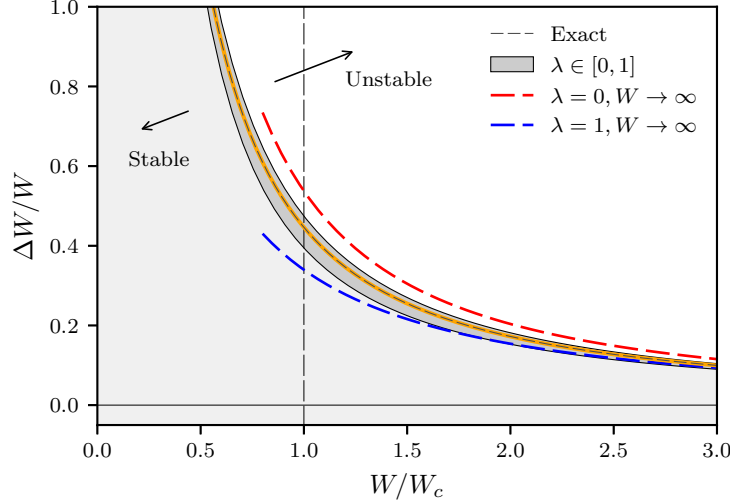


FIGURE 6. Upper and lower bounds, indicated by the dark grey region in the vicinity of the marginal stability curve (thin dashed line). The long dashed lines $\lambda = 0$ and $\lambda = 1$ correspond to asymptotic expressions for the upper and lower bounds, respectively, from (3.7).

$$\frac{dh}{dt} = -\lambda h_0^{5/3} - V^{1/2} (W + \Delta W_* - b_* - t)^{1/2}. \quad (3.1)$$

Along the separatrix curve, h varies monotonically between h_0 and 0, which means that (3.1) with $\lambda \in [0, 1]$ bounds the actual solution to (1.2a). Noting that the system is to be integrated backwards in time from $(b_*, 0)$, $\lambda = 0$ corresponds to neglecting the volume flux in the plume, underestimating the ascent rate of the interface and overestimating the optimal change in wind strength ΔW_* . Conversely, $\lambda = 1$ corresponds to overestimating the volume flux in the plume, overestimating the ascent rate of the interface and underestimating the optimal change in wind strength ΔW_* . In either case, (3.1) provides a good approximation for the small interface heights that occur for large W , because they entail a relatively small volume flux term.

Unlike the original differential equation, (3.1) is readily solved analytically to give

$$h_0 = \lambda h_0^{5/3} \Delta t_* + \frac{2V^{1/2}}{3} (W + \Delta W_* - b_* + t)^{3/2} \Big|_0^{\Delta t_*}, \quad (3.2)$$

where $\Delta t_* = b_* - b_0(1 - h_0)$ is the time it takes the system to reach the unstable fixed point. Equation (3.2) provides the algebraic bounds of the shaded region displayed in figure 6, which exhibits a close agreement with the exact curve for the system's marginal stability, illustrating that the volume flux does not play a significant role in determining the system's stability.

3.2. Asymptotic scaling for $W \rightarrow \infty$

For forward flow (1.3) implies that the buoyancy and interface height at the stable fixed point are, respectively:

$$b_0 = W + W^{2/5} + O\left(\frac{1}{W^{1/5}}\right), \quad h_0 = \frac{1}{W^{3/5}} - \frac{3}{5} \frac{1}{W^{6/5}} + O\left(\frac{1}{W^{9/5}}\right), \quad (3.3)$$

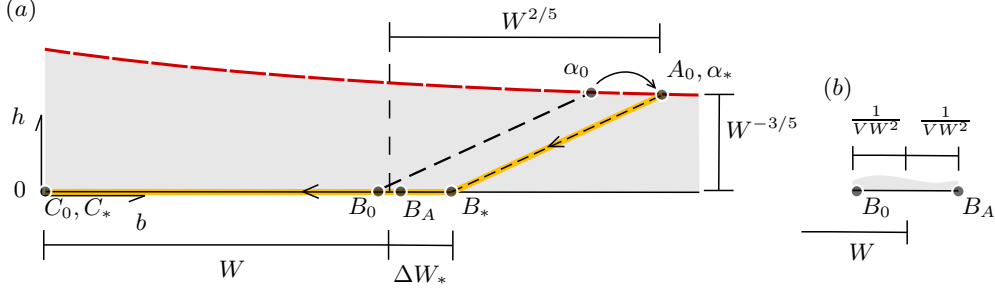


FIGURE 7. The asymptotic representation of phase space (cf. figure 3(b)) for $W \rightarrow \infty$, where (a) depicts the region traversed by the system's trajectory and (b) depicts the relatively small distance between the original unstable fixed point B_0 and the average buoyancy B_A .

for fixed V , which implies that the total buoyancy of the upper layer at the stable fixed point scales according to

$$b_0(1 - h_0) = W + \frac{1}{VW^2} + O\left(\frac{1}{W^{13/5}}\right). \quad (3.4)$$

As $W \rightarrow \infty$ the stable interface height $h_0 \rightarrow 0$ and (2.2), describing the well-mixed interior assumed by Lishman & Woods (2009), indicates that, to leading order, the buoyancy of the stable fixed point for forward flow in a well mixed interior scales in the same way as $b_0(1 - h_0)$:

$$b_m = W + \frac{1}{VW^2} + O\left(\frac{1}{W^{7/2}}\right). \quad (3.5)$$

The buoyancy at the unstable fixed point B_* for reverse flow at wind strength $W + \Delta W_*$, assuming that $\Delta W_* = o(W)$, is:

$$b_* = W + \Delta W_* - \frac{1}{VW^2} + O\left(\frac{1}{W^5}\right). \quad (3.6)$$

Figure 7 illustrates the scaling of the features of phase space when $W \rightarrow \infty$. The interface height is small in comparison with the distance between the stable fixed points for forward and reverse flow. Note that $b \sim (VW)^{-1/2} \rightarrow 0$ is a solution to (1.4) for $W \rightarrow \infty$ and corresponds to a stable reverse flow in which the interior is rapidly flushed by the wind. In order to destabilise forward flow, the buoyancy associated with the unstable fixed point must increase by at least ΔW_* , whose scaling with respect to W we determine below. Recalling that $\Delta t_* = b_* - b_0(1 - h_0)$ from buoyancy conservation, (3.4) and (3.6) imply that $\Delta t_* \sim \Delta W_*$, which, on substitution into (3.2) with (3.3), gives

$$\frac{2V^{1/2}}{3} \Delta W_*^{3/2} + \frac{\lambda}{W} \Delta W_* - \frac{1}{W^{3/5}} \sim 0, \quad (3.7)$$

which is a cubic in $\Delta W_*^{1/2}$ for any given $\lambda \in [0, 1]$. As indicated in figure 6, (3.7) provides a close agreement with the exact bounds obtained in the previous section, even for relatively small values of W . In particular, when $\lambda = 0$, (3.7) provides the useful upper bound:

$$\Delta W_* \sim \left(\frac{3}{2}\right)^{2/3} \frac{1}{V^{1/3}W^{2/5}}. \quad (3.8)$$

More generally, all solutions to (3.7) scale according to $\Delta W_* \sim W^{-2/5}$, which is signifi-

cantly weaker than the scaling $\Delta W_* \sim W^{-2}$ that is implied by (3.4)-(3.6), based on the assumption of a well-mixed interior driven by distributed heating (Lishman & Woods 2009), or a conserved average buoyancy in the case of localised heating.

The asymptotic time scale $\Delta t_* \sim \Delta W_* \sim W^{-2/5}$ is included in figure 5 alongside the lower-bound scaling for $\Delta t_0 \sim W^{-1/2}$ using $\Delta b \sim W$ in (2.4) for large base wind speeds.

4. Energetics for $W \rightarrow \infty$

We will now demonstrate that the scaling (3.8) accounts for the work performed by the wind to homogenise the interior. The optimal increase in wind strength ΔW_* instantaneously reverses the flow. Therefore, over the finite time it takes for the interface to be lowered from $h_0 \ll 1$ to zero, the change in potential energy ΔE_p is:

$$\Delta E_p = \frac{b_0(1-h_0)h_0}{2} + \frac{\Delta t_*}{2} \sim \frac{W^{2/5}}{2}. \quad (4.1)$$

The first term on the right-hand side of (4.1) accounts for lowering the centre of mass of the average buoyancy $b_0(1-h_0)$ by $h_0/2$ and the second term accounts for the buoyancy added to the domain over $\Delta t_* \sim \Delta W_* \sim W^{-2/5}$ at average height $1/2$, which is comparatively small.

The change in the system's potential energy is equal to a fraction $\eta \in [0, 1]$ of the total work ΔE_w undertaken by the wind. To leading order the pressure due to the wind is the base wind strength W and the rate at which the wind performs work on the system corresponds to the product of pressure and volume flux. But, the integral of the volume flux over Δt_* is simply the first term in (3.7), which corresponds to the last term in (3.1) and (3.2):

$$\Delta E_w = \underbrace{W}_{\text{pressure}} \underbrace{\frac{2V^{1/2}}{3}\Delta W_*^{3/2}}_{\text{volume}}. \quad (4.2)$$

Equating $\eta\Delta E_w$ with ΔE_p implies that

$$\Delta W_* \sim \left(\frac{3}{4\eta}\right)^{2/3} \frac{1}{V^{1/3}W^{2/5}}, \quad (4.3)$$

for $W \rightarrow \infty$, which is identical to (3.8) when $\eta = 1/2$. The fraction $\eta = 1/2$ corresponds to the mixing efficiency of high-Rayleigh number convection resulting from heating and cooling at the bottom and top of a domain, respectively (see e.g. Hughes *et al.* 2013, for the particular case of Rayleigh-Bénard convection).

5. Conclusions

The transient response of a stratified interior to sudden changes in the strength of the wind plays a significant role in determining a system's robustness. In particular, the energy required to homogenise a stratified interior makes existing stability estimations based exclusively on a space's average buoyancy overly conservative, especially in the case of large opposing wind strengths.

Two- or multiple-layer stratifications can be produced by a variety of localised sources of buoyancy, besides the point sources considered here. Each would entail a slightly different set of dynamical equations to account for the driven flow's vertical variation in volume flux (see e.g. line plumes in Kaye & Hunt 2004). However, our results are general in suggesting that for moderate to large base wind strengths it is the initial, steady-state,

density profile that is dominant in determining the system's robustness, rather than the particular contribution of volume and heat to the upper layers during the relatively rapid destruction of the stratification.

Further considerations are required to quantify the robustness of a given state more precisely. For example, a low-level opening of finite vertical extent is likely to erode the criterion for stability that we have developed by permitting buoyancy to escape from the interior before the interface reaches floor level (see e.g. Hunt & Linden 2005). On the other hand, the model that we have used assumes that fluid entering the upper layer mixes with the surrounding fluid completely and instantaneously. If relatively cool, dense air descended through the space without mixing significantly with the upper layer, the interface would not be lowered and the critical increase in wind strength might be even larger than our predictions suggest. Whilst such effects are captured phenomenologically by values of η in (4.3) that are less than $1/2$, they warrant further attention.

Acknowledgements

J.C. gratefully acknowledges an Imperial College Junior Research Fellowship.

REFERENCES

- COOMARASWAMY, I. & CAULFIELD, C. 2011 Time-dependent ventilation flows driven by opposing wind and buoyancy. *Journal of Fluid Mechanics* pp. 1 – 28.
- GLADSTONE, C. & WOODS, A. W. 2001 On buoyancy-driven natural ventilation of a room with a heated floor. *Journal of Fluid Mechanics* **441**, 293–314.
- HUGHES, G. O., GAYEN, B. & GRIFFITHS, R. W. 2013 Available potential energy in Rayleigh-Bénard convection. *Journal of Fluid Mechanics* **729**.
- HUNT, G. R. & LINDEN, P. F. 2005 Displacement and mixing ventilation driven by opposing wind and buoyancy. *Journal of Fluid Mechanics* **527**, 27–55.
- KAYE, N. B. & HUNT, G. R. 2004 Time-dependent flows in an emptying filling box. *Journal of Fluid Mechanics* **520**, 135–156.
- LINDEN, P. F. 1999 The fluid mechanics of natural ventilation. *Annual Review of Fluid Mechanics* **31** (1), 201–238.
- LINDEN, P. F., LANE-SERFF, G. F. & SMEED, D. A. 1990 Emptying filling boxes: the fluid mechanics of natural ventilation. *Journal of Fluid Mechanics* **212**, 309–335.
- LISHMAN, B. & WOODS, A. W. 2009 On transitions in natural ventilation flow driven by changes in the wind. *Building and Environment* **44** (4), 666 – 673.
- YUAN, J. & GLICKSMAN, L. R. 2008 Multiple steady states in combined buoyancy and wind driven natural ventilation: The conditions for multiple solutions and the critical point for initial conditions. *Building and Environment* **43** (1), 62 – 69.